Water Resources Research

RESEARCH ARTICLE
10.1029/2020WR027988

Overlooked Implication of Sediment Transport at Low Flow: Migrating Ripples Modulate Streambed Phototrophic and Heterotrophic Microbial Activity

David Scheidweiler[1,2,†], Clara Mendoza-Lera[2,3,†], Michael Mutz[2], and Ute Risse-Buhl[4]

[1]Institute of Earth Sciences, University of Lausanne, Lausanne, Switzerland, [2]Department of Freshwater Conservation, Brandenburg University of Technology Cottbus-Senftenberg, Bad Saarow, Germany, [3]Institute for Environmental Sciences, University of Koblenz-Landau, Landau, Germany, [4]Department River Ecology, Helmholtz Centre for Environmental Research – UFZ, Magdeburg, Germany

Abstract Sandy streambeds are mobile even at low flow velocities at which sediments can be transported as bedload, more specifically as migrating ripples. Small variations in discharge can result in transitions between sediment transport and no-transport. Despite being inherent processes of streams and rivers, the effect of sediment transport and transport regime transition on the phototrophic and heterotrophic activity of streambed microbial communities remains unclear. We performed a microcosm experiment mimicking sediment transport as migrating ripples (i.e., migrating) and no sediment transport (i.e., stationary), and their transition to observe the response of the phototrophic and heterotrophic microbial community. Both net community production and community respiration were respectively 77% and 40% suppressed in migrating sediments compared to stationary sediments. In migrating sediments, a combination of mechanical stress, light limitation, and limited habitable area likely hampered microbial metabolism. Stationary conditions facilitated an active community of phototrophs, mainly diatoms, as indicated by high net community production, high rates of dissolved organic carbon release and silicon retention. After transitioning migrating to stationary and vice versa, differences were maintained regardless of the change in mechanical stress and associated stressors, most likely as a result of the interaction between their antecedent transport conditions and developmental stage that shaped the microbial community. Our results indicate that sediment transported as migrating ripples at low flow velocity can strongly modulate streambed metabolism, and discharge oscillations resulting in sediment transport transitions will result in a mosaic of microbial activity and biomass that will emerge at larger scales determining reach-scale metabolism.

†These authors contributed equally to this work.

Key Points:

- A microcosm approach was used to identify the effect of ripple migration on the metabolism and composition of microbial communities
- Migrating ripples hampered the phototrophic and heterotrophic community respiration, net production, and composition
- The influence of transition from (to) migrating ripple to (from) stationary sediment was modulated by community developmental stage

Supporting Information:

- Supporting Information S1

Correspondence to:
U. Risse-Buhl,
ute.risse-buhl@ufz.de

Citation:
Scheidweiler, D., Mendoza-Lera, C., Mutz, M., & Risse-Buhl, U. (2021). Overlooked implication of sediment transport at low flow: Migrating ripples modulate streambed phototrophic and heterotrophic microbial activity. *Water Resources Research*, *57*, e2020WR027988. https://doi.org/10.1029/2020WR027988

Received 12 JUN 2020
Accepted 28 JAN 2021

1. Introduction

In streams and rivers, ecosystem metabolism (primary production and respiration) that is carried out by multitrophic microbial communities residing mainly in the streambed is shaped by the master variable flow (Battin et al., 2009, 2016; Risse-Buhl et al., 2020). Flow determines both nutrient supply and the sediment transport regime (Hart & Finelly, 1999; Poff et al., 1997). In general terms, sediment transport influences ecosystem metabolism by means of streambed hydromorphology and sediment stability (Atkinson et al., 2008; Uehlinger et al., 2002). The latter one results from the interplay of sediment and flow characteristics (Bridge, 2003). For example, floods are intensive and episodic events that mobilize and scour the entire streambed deeply altering the streambed metabolism and microbial community structure (e.g., O'Connor et al., 2012; Uehlinger, 2000). In contrast, sediment transport at low flow (i.e., flow of water in a stream during prolonged dry weather conditions [Smakhtin, 2001]) is of much less intensity, affecting mainly the finer sediment grain sizes over longer periods (more than half of the year) (Biggs et al., 2005; Bridge, 2003; Singh et al., 2019). Thus, while the former one is a strong shaping force acting episodically on a large temporal scale (once per year [Biggs et al., 2005]), the latter one could potentially shape ecosystem metabolism continuously during much longer periods. However, the implications for ecosystem metabolism of low flow sediment transport are poorly understood.

At low flow, fine to medium sand (grain size ~0.1–0.7 mm) is mobilized and transported as bedload, more specifically as migrating ripples at depth averaged flow velocities of <0.2–0.6 m s^{-1} (Baas, 1999, 2003; Uehlinger et al., 2002; Verdonschot, 2001). Ripple migration is characterized by an erosion-resting cycle (see

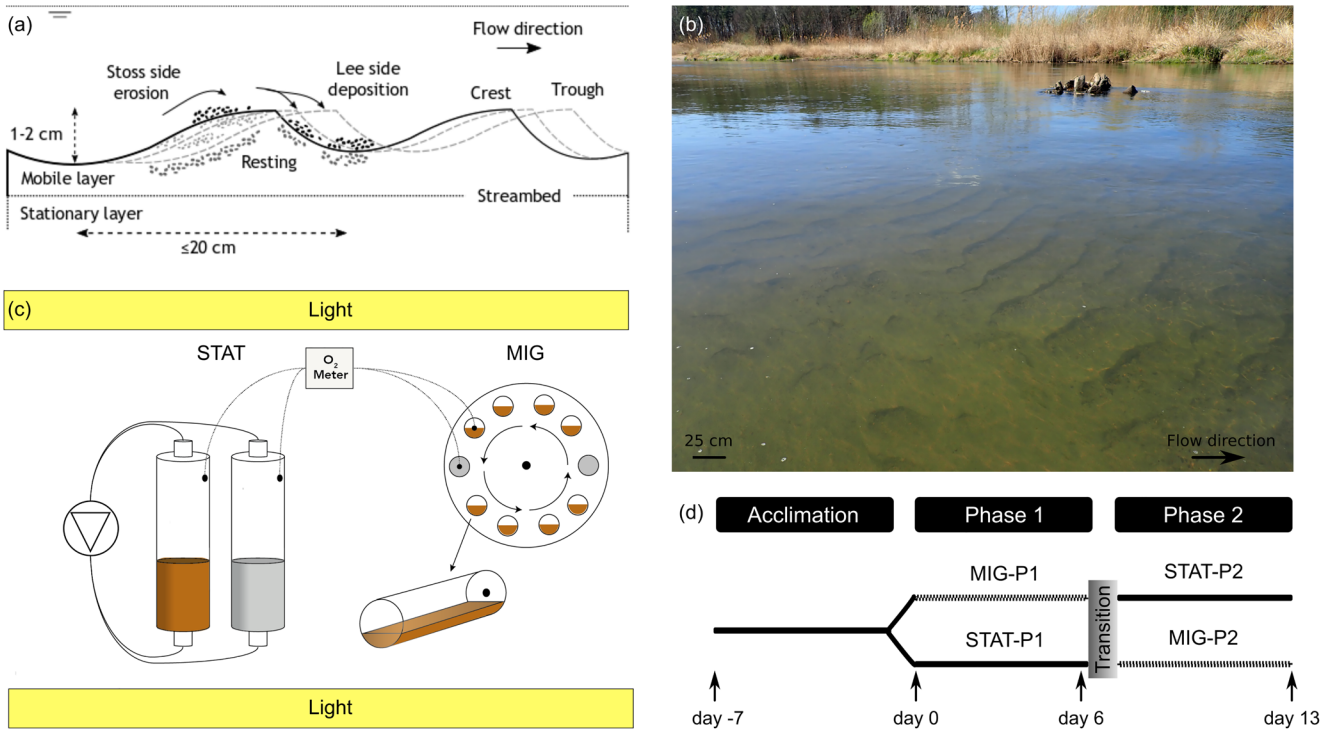

Figure 1. Sediment transport in migrating ripples, patchy streambed with contrasting sediment transport regime and experimental setup. (a) Schematic representation of bedform characteristics and sediment transport in migrating ripples; (b) patchy streambed with migrating ripples and stationary sediment in the River Spree near Cottbus; (c) schematic representation of microcosms that mimicked migrating ripple (MIG) and stationary (STAT) treatments illustrating sediment (brown) and control (gray) microcosms; (d) experimental setup displaying the acclimation phase, the sediment transport regime: migrating ripple (dashed line) and stationary (solid line), and their transition resulting in two experimental phases (phase 1, P1 and phase 2, P2). Arrows indicate the duration of phases and destructive sampling of microcosms (days 0, 6, and 13).

Figure 1a): shear stress erodes sand grains (and other organic particles) at the stoss side and transports them toward the crest, from where they avalanche toward the trough and deposit. There, grains and particles are buried by subsequent grains and remain at rest until the eroding upstream face of the ripple approaches the grain's position, whereupon the erosion-resting cycle starts again. The erosion scales in the range of seconds, whereas the resting phase ranges from several minutes to a few hours according to ripple size and flow velocity (Baas, 1999; Bridge, 2003; Harvey et al., 2012). The time that it takes to transport the entire sediment volume of a ripple is named sediment turnover and is comparable to pore water exchange (Elliot & Brooks, 1997; Savant et al., 1987). Migrating ripples are a common hydromorphological element covering between 20% and 50% of the streambed of a reach (Marcarelli et al., 2015; Mutz et al., 2001; Rabení et al., 2005; Wallbrink, 2004).

Migrating ripples create a unique, complex, and dynamic habitat for multitrophic microbial communities, including heterotrophic bacteria and phototrophs (cyanobacteria and algae). We propose that the uniqueness and complexity of this habitat relay on the combination of promoting and hampering factors. On the one hand, ripples increase mixing of surface and interstitial water (Kaufman et al., 2017; Mendoza Lera & Mutz, 2013; Wolke et al., 2020), supplying the microbial community with oxygen, carbon, and nutrients (Fischer et al., 2005; Zheng et al., 2019). Additionally, migrating ripples play an important role in entrapping and releasing particulate organic matter (Harvey et al., 2012). On the other hand, the migration of sand grains might result in (1) resting times too short to allow the microbial community to grow and differentiate into complex biofilm architectures (Scheidweiler et al., 2019; Sinsabaugh et al., 2015; Zlatanović et al., 2017), (2) burial and thus light limitation for the phototrophs (Pilditch & Miller, 2006), and (3) mechanical stress by grain collision causing cell disruption and biofilm abrasion (Delgado et al., 1991; D. C. Miller, 1989; Probandt et al., 2018). The implications of these factors for ecosystem metabolism have been recently studied for community respiration yet neglecting the phototrophic compartment (Wilczek

et al., 2004; Zlatanović et al., 2017). No direct evidence exists for the effect of ripple migration on phototrophic communities and primary production. Previous research suggests that activity and abundance of phototrophs in sand is lower compared to that in gravel and cobbles (Atkinson et al., 2008; Hoellein et al., 2009; Marcarelli et al., 2015) and in sandy sediment, metabolism is dominated by heterotrophic processes (Marcarelli et al., 2015; Uehlinger et al., 2002). Community respiration is hampered by migrating sand regardless of the organic matter entrapped in the sediment (Zlatanović et al., 2017).

Flow velocity in a given reach is temporally dynamic and spatially heterogeneous even at low flow as a result of channel morphology, changes in discharge and sediment inputs (Baas, 1999; Paola & Seal, 1995). In an ideal stream reach, with well-mixed flow and a single acceleration due to gravity, the boundary shear stress for sand transport are water depth and slope (Bridge, 2003; Leeder, 1982; Leopold et al., 1964). In a lowland reach with a stream gradient of 0.03% (Hünken & Mutz, 2007), small changes in water depth (~4 cm) can result in the transition of sediment transport conditions within hours. While in some areas of the streambed sand is transported as ripples, in other areas sand does not experience movement (i.e., stationary sediment; Figure 1b). Sandy streambeds are thus a mosaic of migrating ripple and stationary habitats experiencing frequent transitions. Therefore, microbial communities inhabiting sand beds experience a transition from sediment migration to stationary and vice versa at a larger temporal scale than the eroding-resting cycle of sand grains in a migrating ripple. To which extent the microbial communities adapt to the new conditions is still unknown, yet research suggests that communities from migrating ripples can adjust to stationary conditions within a few days (Atkinson et al., 2008; D. C. Miller, 1989; Zlatanović et al., 2017).

Our study aimed at determining the effect of (i) sediment transport as occurring in migrating ripples (i.e., mechanical stress and light limitation) and (ii) the transition between ripple migration and stationary conditions on the phototrophic (primary production) and heterotrophic (respiration) activity of a sediment microbial community. We performed a microcosm experiment mimicking ripple migration and stationary sediment, and their transition. First, we hypothesize that under migrating conditions, mechanical stress and light limitation reduces phototrophic and heterotrophic microbial activity, as net community production, community respiration, and bacterial production, by reducing phototrophic biomass and bacterial abundance. Second, we hypothesize that phototrophs are likely more affected than bacteria by migrating ripples due to their larger cell size and dependency on light and thus net community production and phototrophic biomass will be more affected than community respiration and bacterial abundance. Third, we hypothesize that the transition from migrating to stationary and vice versa results in changes of community activity, phototrophic biomass, and bacterial abundance reflecting the antecedent scenarios, for example, activity and biomass/abundance will increase when sediments stop migrating and will decrease when they resume transport as ripples.

2. Materials and Methods

We performed a microcosm experiment under controlled temperature and light conditions in the laboratory. Following a factorial design, we tested the effect of sediment transport and transition of sediment transport regime on the activity of the phototrophic and heterotrophic microbial community of sandy sediments. Our experimental setup follows that of previous studies from Risse-Buhl et al. (2014) and Zlatanović et al. (2017). We mixed the microbial community of migrating ripple and stationary sediments to get an inoculum for the experiment containing phototrophs and heterotrophs. In a first phase, we mimicked sediment transport in the form of migrating ripples and no sediment transport in the form of stationary conditions. In a second phase, microcosms of one treatment were exposed to the opposite treatment conditions to observe the effect of transport regime transition.

2.1. Sediment Sampling and Inoculation

We sampled sandy sediments (D_{50} = 328 μm, D_{10} = 165 μm, and D_{90} = 475 μm, grain sized distribution shown in Figure S1) from a patch of migrating ripples in a second-order lowland stream (Seebach, 52°13′08.5″N, 14°02′27.8″E, Brandenburg, Germany) in November 2014. The stream runs through deciduous forest that is mainly composed of Beech (*Fagus sylvatica* L.), Alder (*Alnus glutinosa* L.), and agricultural landscape before it drains into Lake Scharmützelsee. Approximately 200 mL of sediments were collected from the uppermost

0.5 cm of ripple crest and wet sieved (1 mm–63 μm) to exclude debris, silt, meiofauna and macrofauna. The sediment was placed in 5 L of well aerated and recirculating stream water (sterile filtered through 0.22 μm) that was amended with nutrients to reach mesotrophic conditions (PO_4-P 13 μg L^{-1}; NO_x-N 506 μg L^{-1}; NH_4-N 116 μg L^{-1}; SiO_2-Si 10 g L^{-1}; dissolved organic carbon [DOC] 5 mg C L^{-1}; and dissolved inorganic nitrogen [DIN=NO_x-N+NH_4-N]:soluble reactive phosphorous [SRP] 23).

To obtain a mixed, homogeneous community, we added a microbial community from a stationary sediment to the migrating ripple sediment community. We gently brushed the biofilm from 20 cobbles of the same stream and filtered the suspension through a sieve of 63 μm to remove meiofauna and macrofauna. This community was added to the sampled migrating ripple sediments, which were placed in a climate chamber (Binder, KBW 400, Germany) for acclimation at 12 h light:12 h dark cycle for 7 days. During the light period, sediments received a photosynthetic active radiation of 60 ± 15 μmol m^{-2} s^{-1} (Osram, Lumilux, 18W/865XT 400–700 nm, Germany). The light regime ranges within the saturation irradiance of benthic phototrophic communities (Roberts et al., 2004, and citations therein). The temperature was stepwise increased from 10°C (stream water in situ temperature) to 15°C (experimental temperature) at 1°C for 5 days (see Zlatanović et al., 2017) and stayed at 15°C for the remaining 2 days of the acclimation phase. The overlying water was recirculated with a peristaltic pump (1 L h^{-1}; 520-SN, WatsonMarlow, Cheltenham, UK) to guarantee continuous mixing and oxygen saturation. After the 7 days of acclimation, the sediment was gently mixed before transferring it to the microcosms.

2.2. Experimental Setup

The experimental setup follows a factorial design and mimicked two treatments: migrating ripple and stationary sediments (Figure 1c). The eight microcosms mimicking migrating ripples (MIG) consisted of glass tubes (48 mL, 2.5 cm in diameter, 6.5 cm in length) that were filled with sediment (5.5 mL, corresponding to 3.7 g dry mass, DM) and amended stream water (42.5 mL). The microcosms were closed without headspace and placed horizontally. Sediment depth in migrating ripple microcosms was 0.8 cm at the deepest point. The bottom of the microcosms was shaded using black tape in order to obtain a comparable area of sediment exposed to light in both treatments (18 cm^2). The sediment transport typically observed in migrating ripples was mimicked by horizontally rotating the microcosms around their longitudinal axes (see Figure 1c; Risse-Buhl et al., 2014; Zlatanović et al., 2017). During the rotation, the topmost sand grains avalanched from the brink point to the tube bottom along the sediment heap due to gravity force. Simultaneously, the pore water was exchanged and mixed with the overlying water. One rotation lasted 30 s and sediment turnover was 1 h^{-1}. The experimental frequency of the erosion-resting cycle, sediment turnover, resting time, and exposure to light are all comparable to that of migrating stream ripples (Sukhodolov et al., 2006). As control for microbial activity of the water, one additional microcosm was filled with amended stream water and sterile glass spheres, to match the water volume.

The microcosms mimicking stationary conditions (STAT) consisted of glass syringes (48 mL, 2 cm in diameter, 10.3 cm in length; Optima FORTUNA, Germany), where the 1.7-cm deep sediments (5.5 mL, corresponding to 3.7 g DM) were perfused with amended stream water (Figure 1c). A peristaltic pump ensured a flow against gravity from bottom to top (1.37 mL h^{-1}; Ismatec, Glattbrugg, Switzerland) resulting in a pore water residence time of 53 min, which matched the sediment turnover and hence the pore water residence time of migrating ripple sediments. Thus, our experimental design maintained same pore water exchange and same amount of incorporated organic matter between treatments. As control for microbial activity in the water, an additional microcosm was filled with amended stream water and sterile glass beads (10 mm in diameter) to generate a similar residence time as in the microcosms containing sediments.

All microcosms were kept in a temperature controlled climate chamber at 15°C (Binder, KBW 400, Germany) under a light:dark cycle of 12 h:12 h. Temperature was monitored in additional water-filled microcosms throughout the experiment (HOBO, Onset, Bourne, MA, USA). At day 4 of the experiment, the dissolved oxygen of migrating ripple treatment reached 4 mg L^{-1}. In order to avoid hypoxia and ensure aerobic metabolism, the overlying water was aerated through a sterile metal needle equipped with cellulose acetate filters (0.2 μm pore size) until oxygen saturation avoiding any disturbance of the sediment.

The experiment consisted of two phases simulating the dynamics of the streambed in terms of sediment transport (Figure 1d):

1. In phase 1 (P1), we studied the effect of migrating ripples on the phototrophic and heterotrophic microbial activity ($n = 8$). The microcosms run for 6 days as MIG-P1 and STAT-P1 treatments. At day 6, four random replicates of each treatment were retrieved, opened, and destructively sampled for further analyses.
2. In phase 2 (P2), we observed the effect of transport regime transition. We transferred the remaining microcosms to the opposite treatment, that is, MIG-P1 sediments were placed in syringes for stationary conditions (STAT-P2), and in turn STAT-P1 sediments were placed in glass tubes under migrating ripple conditions (MIG-P2). The transition of sediments to the opposite microcosms was done within 4 h. New amended stream water was added to each microcosms. Microcosms ($n = 4$) were incubated for another 7 days and the remaining four replicates of each treatment were opened and destructively sampled at day 13.

Response variables for microbial activity were net community production (NCP), community respiration (CR), bacterial production (BP), and dissolved inorganic nutrients and dissolved organic carbon retention and release. Phototrophic biomass (Chlorophyll *a* [Chl *a*] and additional photosynthetic pigments) and bacterial abundance were determined as descriptors for the microbial community in sandy sediments. Net community production and community respiration were measured as changes in oxygen concentration during light and dark periods every day. All other parameters were analyzed after opening and destructively sampling the microcosms at days 0, 6, and 13.

2.3. Sediment Community Activity

All microcosms were equipped with one optode spot (PreSens GmbH, Regensburg, Germany) to monitor oxygen concentrations every 15 min (Oxy10, PreSens GmbH). Oxygen concentration varied between 4.7 and 14.4 mg L^{-1} in migrating ripple microcosms and between 7.0 and 13.9 mg L^{-1} in stationary microcosms. The decrease of oxygen concentration averaged 0.9 mg L^{-1} over all replicates, treatments, and phases during the dark period. During the light period, the increase of oxygen concentration averaged 1.4 mg L^{-1}, except in MIG-P1 where oxygen concentration decreased by 0.3 mg L^{-1}. Microbial communities adjusted to the microcosm conditions for 20 h. Data of the first 2 h after changing the light regime were excluded (Macedo et al., 1998).

For the migrating ripple treatment, net community production (NCP; Equation 1) and community respiration (CR; Equation 2) of the sediment were calculated as

$$NCP_{MIG} = \left(\left(\frac{dC_{light}}{dt}\right) - \left(\frac{dC_{control,light}}{dt}\right)\right) \times \left(\frac{V}{DM}\right) \quad (1)$$

$$CR_{MIG} = \left(\left(\frac{dC_{dark}}{dt}\right) - \left(\frac{dC_{control,dark}}{dt}\right)\right) \times \left(\frac{V}{DM}\right) \quad (2)$$

where dC/dt is the change of oxygen concentration in time (mg O_2 L^{-1} h^{-1}), the subscripts light and dark correspond to the light period and control to the control microcosms, V is the volume of water in microcosms (L), and DM is the sediment dry mass (g, see details below).

In the stationary treatment, oxygen concentration did not reach a steady plateau during the light or dark period due to the low flow rate and related water mixing in the microcosm. Thus, measured oxygen concentrations were fitted to an exponential decay model (see supporting information Text S2 and Figure S2) and the steady state concentrations C_{light} and C_{dark} were then used to estimate net community production (NCP; Equation 3) and community respiration (CR; Equation 4) as

$$NCP_{STAT} = \left(C_{light} - C_{control}\right) \times \left(\frac{Q}{DM}\right) \quad (3)$$

$$CR_{STAT} = \left(C_{control} - C_{dark}\right) \times \left(\frac{Q}{DM}\right) \quad (4)$$

where $C_{control}$ is the mean oxygen concentration in the control microcosms over 4 h after the seventh hour of a light period, Q is the flow rate (L h^{-1}).

Bacterial production (BP) was estimated from sediment subsamples (0.5 mL) as the incorporation of radiolabeled [^{14}C]leucine (50 μM final concentration; MP Biomedicals, Santa Ana, CA) into proteins following Buesing and Gessner (2006) and Attermeyer et al. (2013). The samples were incubated for 60 min at 15°C and reactions were stopped by adding trichloroacetic acid (TCA, 5% final concentration). Controls consisted of parallel samples inactivated with TCA before [^{14}C]leucine was added. The activity of the extracted protein was determined by a scintillation counter (Packard Tri-Carb 1600CA) and converted into moles of leucine incorporated per hour per gram DM. The rate of carbon produced was estimated following Buesing and Gessner (2006).

2.4. Sediment Community Descriptors

To determine phototrophic biomass via photosynthetic pigments (Chlorophyll *a* and *b*, fucoxanthin, and pheophytin *a* and *b*), sediment subsamples (3 mL) from each microcosm were stored at −20°C before extraction with ethanol (99%) and several freeze–thaw cycles. Analysis were then performed by high-performance liquid chromatography using a reversed-phase column (YMC C30, particle size 3 μm, 250 × 2 mm, Sepserv, Berlin) equipped with an ASI-100 auto sampler, a P680 pump, and a diode array detector PDA100, connected to the Chromeleon software (DIONEX, 2005). Twenty microliters of extract was injected in the column, in which the gradient elution (eluent A: 450 mL methanol, 200 mL acetonitrile, 300 mL HPLC-water and 50 mL ion-pair reagent; eluent B: 300 mL methanol, 500 mL acetonitrile and 200 mL ethylacetate) was maintained at 35°C with a flow of 0.3 mL min^{-1}. Pigments were calibrated using standards from the DHI Water and Environment Institute (Hørsholm, Denmark).

Bacterial abundance was estimated from sediment subsamples (1 mL) that were fixed with formaldehyde (final concentration 2%). Cells were extracted from the sediment by sonication (2 times á 2 min at 60% power; Transonic Digital Type T790/H; Elma, Singen, Germany), concentrated on 0.2 μm black polycarbonate membranes (Nuclepore; Whatman, Germany) and stained using 4′,6-di-amidino-2-phenylindole following the protocol of Nixdorf and Jander (2003). At least 400 bacterial cells were scanned by epifluorescence microscopy (Axioskop Zeiss 1000X; Zeiss, Jena, Germany) in randomly selected squares ($n > 30$). Production rates of photosynthetic pigments and growth rates of bacteria were calculated respectively as increase in biomass or abundance from day 0 to day 6 for phase 1 and from day 6 to day 13 for phase 2.

A sediment subsample (1 mL) from each microcosm was dried till constant mass at 60°C for DM determination and then combusted to obtain ash-free dry mass (AFDM; 4 h, 500°C). All community descriptors are represented per g DM of sediment.

2.5. Dissolved Organic Carbon and Inorganic Nutrient Concentrations

The water from migrating microcosms was collected at day 6 and day 13 representative for phases 1 and 2, respectively. The outflowing water from the stationary microcosms was collected daily between days 1–6 and days 7–13 to obtain a composite sample over each phase. Background concentrations were determined from control microcosms. Water samples were filtered (prewashed 0.45 μm cellulose acetate filters; Sartorius, Göttingen, Germany) and stored at −20°C for later analysis. DOC was measured with a total organic carbon analyzer (Shimadzu, Tokyo, Japan). SRP, NO_x-N, NH_4-N, and SiO_2-Si were determined spectrophotometrically by a segmented flow injection analyzer (PERSTORP Analytical, Rodgau, Germany) and UV/VIS spectrometer (Perkin Elmer, Rodgau, Germany), respectively, according to standard methods (DEV, 1976–2009). Concentration data were used to calculate the percental difference between control and treatment and the molar ratio of dissolved inorganic nitrogen (DIN = NO_x-N + NH_4-N) to SRP. DOC and dissolved nutrients were corrected for control concentrations and expressed as daily loads taking into consideration

the total volume of water that was in the microcosms for each phase (MIG 40 mL, STAT-P1: 198 mL, and STAT-P2: 231 mL). Negative values indicate retention and positive values indicate release.

2.6. Statistics

All statistical tests and graphics were performed in R (version 3.6.2; R Core Team, 2018). For graphical presentation, we used the package "ggplot2" (Wickham, 2009). Daily data of metabolism of each experimental phase were used to calculate the intercepts at days 6 and 13 (NCP and CR) and their slopes during each phase (NCP dynamics and CR dynamics). Outliers defined as data points outside the 2 times inter quartile range were excluded from graphical presentation and statistical tests of the metabolism data set. Between 1 and 2 values per parameter were excluded and number of replicates per treatment and phase was 3–8. Linear mixed effects models were used for assessing the effect of sediment transport (ST), transport regime transition (TR), and their interaction (ST × TR; fixed effects) on intercepts and slopes of NCP and CR (response variables), with replicate as random factor using the *lmer* function (package "lme4" [Bates et al., 2015]; full model: response variable ~ ST × TR + [1|replicate]). *p*-Values were obtained by likelihood ratio tests of the full model with the effect in question against the model without the effect in question (reduced model to test for sediment transport effect: response variable ~ TR + [1|replicate]; to test for transport regime transition effect: response variable ~ ST + [1|replicate]; to test for interaction: response variable ~ ST + TR + [1|replicate]). Linear models were performed to assess effects of sediment transport, transport regime transition, and their interaction on bacterial production and microbial community descriptors using the *lm* function (response variable ~ ST × TR). For all models, pairwise comparisons were performed using *emmeans* function (package "emmeans," Lenth, 2020). Differences were considered significant at $p < 0.05$. Visual inspection of residual plots did not reveal any obvious deviations from homoscedasticity or normality.

3. Results

3.1. Metabolism

Average net community production and community respiration as well as their dynamics were significantly affected by both sediment transport and transport regime transition (Figure 2). Their significant interaction indicated that microbial communities responded differently to sediment transport depending on the experimental phase. Before the transition (phase 1), net community production and community respiration were respectively 77.0% and 39.7% lower in migrating sediments compared to stationary sediments (Figures 2a and 2c). Both net community production and community respiration were highly variable between the replicates of the stationary treatment STAT-P1 (coefficient of variation: 0.70 and 0.34, respectively) in comparison to the migrating treatment MIG-P1 (0.29 and 0.13, respectively). The dynamics of net community production (Figures 2b and S3) showed a general increase over time during phase 1, which was more pronounced for stationary sediments (3.1 times higher than migrating treatment). On the contrary, community respiration dynamics decreased over time for both treatments at comparable rates.

After the transition (phase 2), metabolism showed the opposite response to sediment transport than in phase 1. Net community production and community respiration were respectively 31.4 times and 2.5 times higher in migrating than in stationary sediments of phase 2 (Figures 2a and 2c). The dynamics of net community production showed a general increase for both treatments, which was higher for the migrating than for the stationary sediments (Figures 2b and S3). Community respiration dynamics showed an increase over time for migrating and a decrease for stationary sediments (Figure 2d).

The transport regime transition (i.e., MIG-P1 to STAT-P2 and STAT-P1 to MIG-P2) did not affect net community production, community respiration, or net community production dynamics (Figures 2a–2c) but significantly affected community respiration dynamics (Figure 2d). Despite significantly different community respiration dynamics, community respiration was comparable between MIG-P1 and STAT-P2 as well as between STAT-P1 and MIG-P2. Comparing the treatments over both phases, net community production and community respiration in MIG-P2 were respectively 10.5 times and 2.7 times higher compared to MIG-P1. STAT-P2 had 10.4 times lower net community production compared to STAT-P1, whereas community respiration was comparable between the two phases of this treatment.

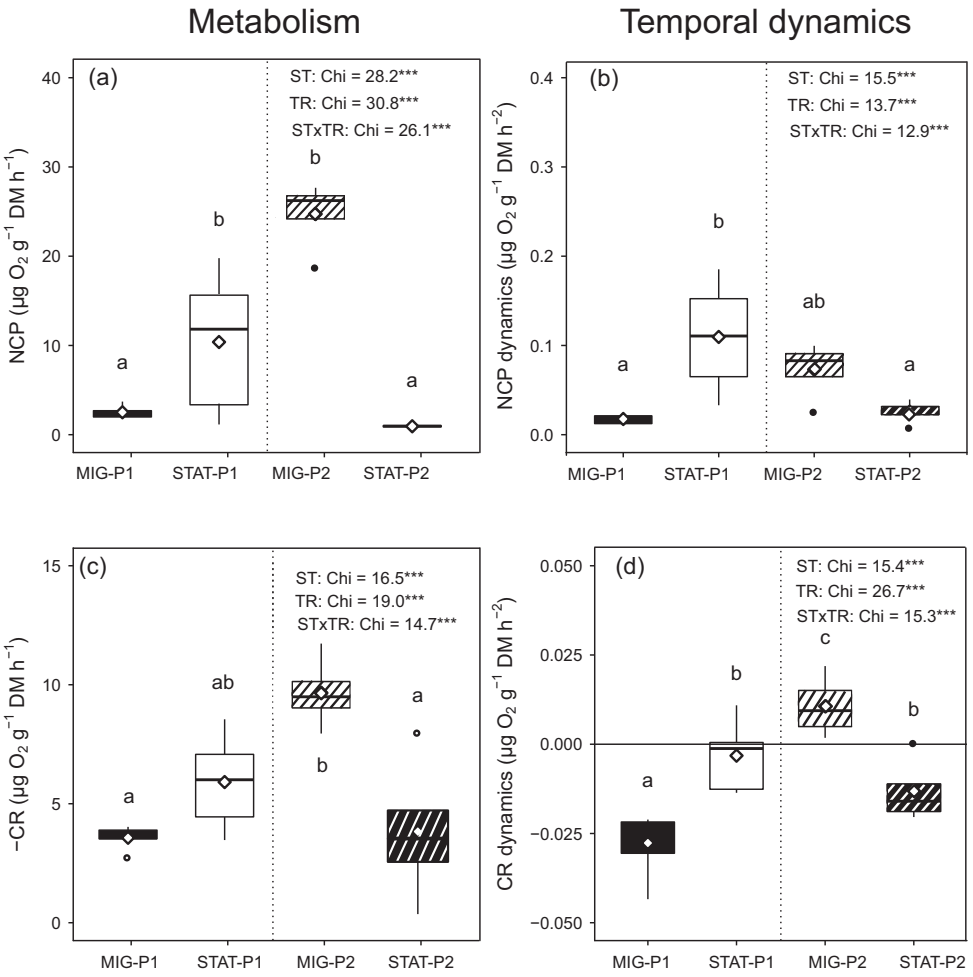

Figure 2. Boxplots displaying the effect of sediment transport and transport regime transition on the activity of the sediment community. (a and b) Net community production (NCP) and (c and d) community respiration (CR) of migrating ripple (MIG) and stationary (STAT) sediments of phase 1 (P1) and phase 2 (P2) after transport regime transition. Daily data of NCP and CR of each phase are shown in Figure S3. Vertical dashed line separates experimental phases. Description of boxes: top and bottom edge represent 75th and 25th percentile, respectively, solid line bisecting the boxes represents the median, the diamond represents the mean, and ends of whiskers represent the 90th and 10th percentile and black dots represent data points outside the 90th and 10th percentile (n = 3–8). Chi revealed form likelihood ratio tests for effects of sediment transport (ST, df = 2), transport regime transition (TR, df = 2), and their interaction (ST × TR, df = 1) are displayed in each plot. Different lower-case letters (a, b, c, ab) above boxes indicate significant differences between treatments and phases ($p < 0.05$); similar letters indicate no significant difference ($p > 0.05$).

3.2. Microbial Community Descriptors and Bacterial Production

At the beginning of phase 1, Chl *a* content was 0.38 ± 0.06 µg g^{-1} DM (Table 1). Fucoxanthin was the dominant pigment and estimated 48.4% of Chl *a*. Chl *b* content was low and represented less than 5% of Chl *a* (Table 1). Pheophytin *a* and *b* were detected at low concentrations of <0.03–0.09 µg g^{-1} DM or below the detection limit throughout the experiment.

Chl *a* ranged between 0.41 and 1.03 µg g^{-1} DM throughout the experiment. Fucoxanthin was the dominant pigment and made up between 39.6% and 53.8%, whereas Chl *b* ranged between 3.3% and 14.4% over both phases. Chl *b* was affected neither by sediment transport nor by transport regime transition. Sediment transport significantly affected Chl *a* (t-value = 5.06, $p < 0.001$) and fucoxanthin (t-value = 6.92, $p < 0.001$). The significant interaction indicated that sediment transport effects on Chl *a* (t-value = −4.47, $p < 0.001$) and fucoxanthin (t-value = −6.28, $p < 0.001$) differed depending on the experimental phase. For phase

Table 1
Initial Microbial Community Composition in Sediments at the Beginning of Phase 1

Descriptor	Unit	Mean ± SD (n = 4)
Chl *a*	μg g^{-1} DM	0.38 ± 0.06
Chl *b*	μg g^{-1} DM	0.05 ± 0.01
Fucoxanthin	μg g^{-1} DM	0.18 ± 0.05
Bacteria	cells g DM^{-1}	$8.3 \times 10^7 \pm 0.9 \times 10^7$
BP	μg C g^{-1} DM h^{-1}	22.98 ± 2.73
Specific BP	pg C $cell^{-1}$	0.32 ± 0.03

Note. BP, bacterial production; SD, standard deviation.

1, no differences were observed among sediments for the two pigments (Figures 3a–3c). However, during phase 2, both Chl *a* and fucoxanthin increased in migrating sediments (MIG-P2) resulting in 1.8 times higher concentrations compared to stationary sediments. The transition from migrating to stationary did not affect Chl *a* or fucoxanthin, while the transition from stationary to migrating resulted in 1.3 times and 1.4 times higher Chl *a* and fucoxanthin. Chl *a* and fucoxanthin in stationary sediments were comparable between phases.

Bacterial abundance ranged between 3.98×10^7 and 1.04×10^8 cells g^{-1} DM and was significant negatively affected by sediment transport (t-value = −3.99, p = 0.002, Figure 3d). Sediment transport effects were similar between phases as confirmed by the missing significant interaction (t-value = −1.55, p = 0.15). In both phases, bacteria were less abundant in migrating than in stationary sediments. Additionally, the transition from stationary to migrating resulted in 47.3% lower bacterial abundance, while no changes occurred in the transition from migrating to stationary.

AFDM increased throughout the experiment from initially 1.98 ± 0.13 to 2.49 ± 0.17 mg AFDM g^{-1} DM at day 13. However, sediment transport did not significantly affect AFDM (t-value = 1.09, p = 0.30).

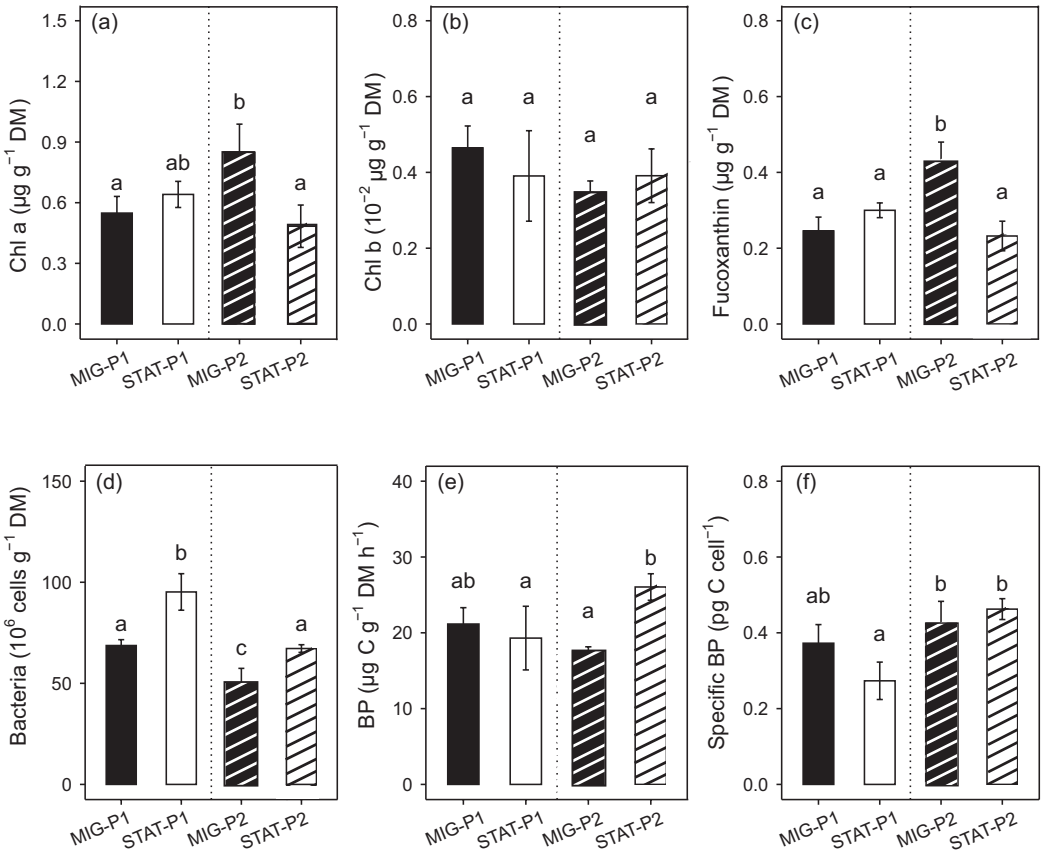

Figure 3. Effects of sediment transport and transport regime transition on microbial community descriptors and bacterial production. (a) Chl *a*, (b) Chl *b*, (c) fucoxanthin, (d) bacterial abundance, (e) bacterial production (BP), and (f) specific bacterial production displaying the production per bacterial cell (mean ± SD, n = 3–4) in migrating ripple (MIG) and stationary (STAT) sediments of phase 1 (P1) and phase 2 (P2) after transport regime transition. Vertical dotted line separates experimental phases. Different lower-case letters (a, b, c, ab) above boxes indicate significant differences between treatments and phases ($p < 0.05$); similar letters indicate no significant difference ($p > 0.05$).

Table 2
Phototrophic Biomass Production (μg g^{-1}DM h^{-1}) and Bacterial Growth Rates (Cells g^{-1}DM h^{-1}) in Migrating Ripple (MIG) and Stationary (STAT) Sediments of Phase 1 (P1) and Phase 2 (P2) After Transport Regime Transition (Mean ± SD, n = 4)

	Phase 1 (0–6 days)		Phase 2 (7–13 days)		
	MIG-P1	STAT-P1	MIG-P2	STAT-P2	LM results
Chl *a*	$1.17 \times 10^{-3} \pm 0.57 \times 10^{-3}$	$1.82 \times 10^{-3} \pm 0.45 \times 10^{-3}$	$1.25 \times 10^{-3} \pm 0.82 \times 10^{-3}$	$-3.87 \times 10^{-4} \pm 6.24 \times 10^{-4}$	ST, ST × TR
Chl *b*	$-2.92 \times 10^{-5} \pm 4.01 \times 10^{-5}$	$-8.06 \times 10^{-5} \pm 8.29 \times 10^{-5}$	$-2.56 \times 10^{-5} \pm 1.78 \times 10^{-5}$	$-4.37 \times 10^{-5} \pm 4.22 \times 10^{-5}$	ns[a]
Fucoxanthin	$4.28 \times 10^{-4} \pm 2.54 \times 10^{-4}$	$8.06 \times 10^{-4} \pm 1.35 \times 10^{-4}$	$7.46 \times 10^{-4} \pm 3.25 \times 10^{-4}$	$-0.79 \times 10^{-4} \pm 2.32 \times 10^{-4}$	ST, ST × TR
Bacteria	$-9.96 \times 10^{-4} \pm 2.01 \times 10^{-4}$	$8.44 \times 10^{-4} \pm 6.27 \times 10^{-4}$	$-0.27 \times 10^{-4} \pm 4.33 \times 10^{-4}$	$-8.89 \times 10^{-3} \pm 0.11 \times 10^{-3}$	ST, TR

Note. Significant results ($p < 0.05$) of the linear model (LM) are represented by upper case letters for sediment transport (ST), transport regime transition (TR), and their interaction (ST×TR).
[a]ns, no significant effects.

3.3. Biomass Production and Nutrient Dynamics

Chl *a* increased in both migrating and stationary sediments during phase 1 (Table 2). During phase 2, Chl *a* further increased in migrating sediments, while it decreased in stationary sediments. Production of fucoxanthin mirrored patterns of Chl *a*. Bacterial growth rates in migrating sediments of both phases were negative, whereas in STAT-P1 sediments bacterial growth rates were positive (Table 2). In STAT-P2, growth rates of bacteria were less negative than in migrating sediments.

Sediment transport affected bacterial production (t-value = −4.73, $p < 0.001$); however, this difference arises from differences observed in phase 2 but not in phase 1 (Figure 3e). Specific bacterial production was not affected by sediment transport (t-value = −1.12, $p = 0.29$), but by transport regime transition (t-value = −5.25, $p < 0.001$) and was higher in phase 2 compared to phase 1 (Figures 3e and 3f). For phase 1, the differences in bacterial abundance and production between migrating and stationary sediments resulted in comparable specific bacterial production (Figure 3e).

Considering solute dynamics, we are aware that changes in loads were driven by both, biological and physical processes. Using the same sediment volume in all microcosms allowed comparing sediment transport conditions and their transition. Daily DOC loads responded differently to sediment transport with respect to transport regime transition (treatment: t-value = −3.50, $p = 0.003$) (Table 3). DOC was released from STAT-P1 and retained in STAT-P2 sediments. SRP was released from both migrating sediments at higher rates compared to both stationary sediments (treatment: t-value = −6.05, $p < 0.001$). Overall, NH_4-N was retained except for STAT-P2 where it was released. More NH_4-N was retained in MIG-P1 than in STAT-P1 (treatment: t-value = 3.21, $p = 0.005$) at a comparable rate between phases. Except for MIG-P1, NO_x-N was

Table 3
Daily Rates of Retention and Release of Dissolved Organic Carbon (DOC) and Dissolved Inorganic Nutrient Loads and Molar Ratio DIN:SRP of Migrating Ripple (MIG) and Stationary (STAT) Sediments of Phase 1 (P1) and Phase 2 (P2) After Transport Regime Transition (Mean ± SD, n = 4–8)

	Phase 1 (days 0–6)		Phase 2 (days 7–13)		
	MIG-P1	STAT-P1	MIG-P2	STAT-P2	LM results
DOC (μg day^{-1})	1.61 ± 7.33 (5%)	28.42 ± 35.18 (20%)	5.03 ± 2.49 (22%)	−49.09 ± 17.72 (−20%)	ST × TR
SRP (μg day^{-1})	0.351 ± 0.133 (1,012%)	−0.002 ± 0.045 (−1%)	0.222 ± 0.161 (292%)	0.021 ± 0.018 (19%)	ST
N-NH_4 (μg day^{-1})	−0.36 ± 0.06 (−65%)	−0.22 ± 0.09 (−37%)	−0.35 ± 0.04 (−55%)	0.75 ± 0.02 (227%)	ST, ST × TR
N-NO_x (μg day^{-1})	0.82 ± 0.60 (27%)	−5.19 ± 0.85 (−34%)	−2.08 ± 0.37 (−64%)	−6.06 ± 2.58 (−60%)	ST, TR
Si-SiO_2 (μg day^{-1})	−19.00 ± 3.90 (−27%)	−41.52 ± 5.77 (−12%)	−23.33 ± 3.75 (−35%)	−28.00 ± 8.16 (−9%)	ST, ST × TR
DIN:SRP	5.5 ± 2.3	40.1 ± 14.8	3.9 ± 4.4	18.9 ± 10.3	ST

Note. Values in parentheses indicate the change in concentration with respect to the control. Significant effects ($p < 0.05$) of the linear model (LM) are represented by upper case letters for sediment transport (ST), transition (TR), and their interaction (ST × TR).
Abbreviation: DIN, dissolved inorganic nitrogen.

overall retained what resulted in differences between phases and overall the release or retention was lower in migrating sediments compared to stationary sediments. Sediment transport significantly affected SiO_2-Si (treatment: t-value $= -6.45$, $p < 0.001$), where less SiO_2-Si was retained in migrating than in stationary sediments for both phases.

4. Discussion

Our study reveals that even at low flow, sediment transport and its dynamics (i.e., transport regime transition) modulates streambed metabolism by not only affecting the activity of the heterotrophic community, but also that of the phototrophic community. This is, to the best of our knowledge, the first study to address this overlooked aspect in streams and rivers. Given the large temporal extent (>50%) of low stream flow periods during the year (Baas, 2003; Singh et al., 2019), our findings contribute to better understand the temporal variability of metabolism and nutrient cycling between and within reaches during low flow periods at a velocity range of <0.2–0.6 m s^{-1}. Such low flow periods were observed to dominate the annual flow at the majority of the 3,600 gauging stations covering streams and rivers in England and Wales (Booker & Dunbar, 2008) and at 12 of 22 gauging stations at larger rivers in the United States (Verzano et al., 2012). Based on the worldwide heavy catchment erosion and increased sand inputs, migrating ripples may become even more common (Sutherland et al., 2010; Wood & Armitage, 1997). Furthermore, our results highlight that the response of the sediment microbial community to sediment migration is conditioned by the antecedent conditions the microbial community experienced. At the reach scale, ecosystem function of sand bed streams is thus a product of the community responses to current sediment transport and the legacy of the transitions between migration and stationary.

4.1. Phototrophic and Heterotrophic Microbial Activity Modulated by Migrating Ripples (Phase 1)

In accordance with our first hypothesis, mechanical stress and light attenuation induced by ripple migration reduced overall metabolism. This expands previous findings limited to heterotrophic communities (e.g., Wolke et al., 2020; Zlatanović et al., 2017). In similar microcosms to ours, Zlatanović et al. (2017) reported an overall 38.0%–65.7% lower respiration in migrating ripples (turnover 2 h^{-1}) compared to stationary sediments. Despite a longer resting time in migrating ripple sediments of our experimental approach (turnover 1 h^{-1}), community respiration was 39.7% lower compared to stationary sediments. Similar results have been revealed from modeling as well as from flume experiments simulating stream bedforms and continental shelf bedforms (Ahmerkamp et al., 2015, 2017; Wolke et al., 2020; Zheng et al., 2019). For example, respiration in German Bight sediments is 55.6%–78.9% lower at stations with migrating bedforms than at stations with stationary bedforms (Ahmerkamp et al., 2017). In flumes simulating stream bedforms, oxygen uptake was 50.4%–70.7% lower at the highest bedform migration velocity of 0.19 mm s^{-1} (equivalent to a turnover of 4.8 h^{-1}) than in stationary ripples (Wolke et al., 2020). In contrast to these studies, we included the phototrophs in our observation showing that also net community production is hampered by ripple migration (77.0%). Phototrophs added more complexity allowing a community with different trophic levels, still the effects of sediment transport are maintained.

In streams and rivers, time for one full sediment turnover of a migrating ripple depends on bedform migration velocity and ripple length. Bedform migration velocity scales with bed shear stress (0.014–0.7 m h^{-1}) (Lichtman et al., 2018); ripple length scales with grain size (0.03–0.65 m) (Charru et al., 2013) and is further variable among ripple planforms (three-dimensional linguoid, two-dimensional straight-crested, and sinuous-crest) (Baas, 1993). Hence, sediment turnover of migrating ripples in streams and rivers varies from once per several minutes to once per few hours. The sediment turnover of 1 h^{-1} in our microcosm experiment corresponds to a ripple length of 16 cm (fully developed migrating ripple at the corresponding grain size) (Baas, 1993) and to a bedform migration velocity of 0.44 mm s^{-1} (average bedform migration velocity observed for biologically colonized sandy sediments) (Lichtman et al., 2018). This beform migration velocity is in the lower range of that reported for pure and biologically colonized sand observed in hydraulic flumes (Baas, 1993; Elliot & Brooks, 1997; Wolke et al., 2020; Zheng et al., 2019). Though further research is needed, we expect that at continuous ripple migration and/or at faster sediment turnover than in our microcosm experiment (1 h^{-1}) and in the experiment of Zlatanović et al. (2017) (2 h^{-1}) will have similar or

even more pronounced negative effects on both net community production and community respiration. For instance, with increasing sediment turnover, Wolke et al. (2020) reported decreasing oxygen uptake rates, and D. C. Miller (1989) reported decreasing bacteria and diatom abundance. Whereas at slower sediment turnover, that allows growth of heterotrophs and phototrophs, other response patterns can be expected. Dunes for instance, either stationary or migrating, have been shown to have high oxygen uptake rates, bacterial production, and abundance (Rutherford et al., 1991, 1993; Wilczek et al., 2004). This trend toward increased respiration with decreasing sediment turnover suggests that the influence of sediment migration is linked to mechanical stress.

Although resuspension and downstream transport of microbial cells as a result of sediment transport (Risse-Buhl et al., 2014; Shimeta et al., 2002) can reduce the metabolism in migrating ripples, this effect has been excluded in our setup. Further, our experimental approach maintained the same pore water exchange and same content of organic matter between treatments. Thus, we propose that the observed reduced metabolic activity in migrating ripple compared to stationary sediments resulted mainly from three factors associated with mechanical stress: physical abrasion, habitable area, and/or light limitation.

Rolling and/or sliding sediment grains colliding with microbial cells can cause both cell damage and biofilm abrasion, as observed by raster electron microscopy on diatom shells (Delgado et al., 1991; D. C. Miller, 1989). These authors discussed that diatoms may have specific physiological adaptations to withstand cell breakage as potential survival strategy, for example, heavier frustules or production of extra mucus. Moreover, small diatom taxa (<50 μm) can remain in sediment depressions where they are protected from the physical abrasion (Jewson et al., 2006; Krejci & Lowe, 1986; A. R. Miller et al., 1987). Similarly, the small cell size of bacteria (1 μm) allows them to develop in sheltered areas at sand grains such as depressions, fissures, and crevices where they are less exposed to physical abrasion (Ahmerkamp et al., 2020; Probandt et al., 2018; Weise & Rheinheimer, 1978). Thus, mechanical stress could have acted as a selective force limiting the community to the "habitable" area of sand grains. In stationary sediment, the "habitable" area extends to almost the entire surface area of sand grains (except for the contact area among grains), allowing a more abundant microbial community. This difference was likely enhanced by the flow-through setup that ensured supply of solutes to the entire surface area. For example, Mendoza-Lera et al. (2017) showed that higher advective supply of nutrients enhances the area colonizable by the microbial community. The absence of sediment transport and presence of advective supply of nutrients, carbon, and oxygen likely allowed phototrophs and bacteria to arrange themselves into complex architectures through the sediment pores (Risse-Buhl et al., 2017, 2020; Scheidweiler et al., 2019). This arrangement is known to promote emergent properties, which are not observable for instance in free-living bacterial cells including more efficient use of resources (Flemming et al., 2016). In line with this, the retention of nitrate and the high DIN:SRP ratio indicated efficient resource utilization in stationary sediments compared to migrating ones. In fact, stationary ripples are more efficient in removing nitrate than migrating ones (Zheng et al., 2019), pointing out to the key effect of mechanical stress. Moreover, rates of DOC release indicate an active phototrophic community producing exudates which further promote heterotrophic activity (e.g., Espeland & Wetzel, 2001; Romaní & Sabater, 2000; Sobczak, 1996). Sediment stability likely facilitated hot spots of heterotrophic activity in their proximity utilizing labile DOC, all resulting in high metabolic rates.

The microcosms were arranged in order to ensure the same light availability over both sediment transport conditions. In stationary sediment, the phototrophic community likely established in the photic sediment layer, which was approximately 2 mm deep (own measurements, data not published). In contrast, the ripple sediment periodically migrated (1 h^{-1}) burying phototrophs within the sand heap, which were likely light limited. Diatoms were the most abundant phototrophs as revealed by the high abundance of fucoxanthin and by the high retention of soluble silicate, which is one of the necessary resources for producing the diatom frustule (see Kohl & Nicklisch, 1988). Motility of diatoms is advantageous to overcome burying and light limitation (Dickman et al., 2005; Izagirre et al., 2009). Diatoms are described to move at velocities of 0.6–36 mm h^{-1} (Cohn & Weitzell, 1996; Consalvey et al., 2004; Hay et al., 1993). Given this velocity range, diatoms would need between 2 min and 13 h to reach the photic sediment surface considering a sediment depth of a few grains (edges of the sand heap) to a maximum of 0.8 cm (center of sand heap). As microcosms were resting for 1 h, it is reasonable to assume that a fraction of diatoms remained buried and needed to cope with the limiting light conditions. Along this line, diatoms typically dominated dark grown biofilms

(Izagirre et al., 2009; Sekar et al., 2002). Certain species of diatoms can switch their metabolism from photoautotrophy toward heterotrophy respiring exogenous sugars or nitrate (Kamp et al., 2011; Lewin & Lewin, 1960; Villanova et al., 2017; Vincent & Goldman, 1980). In this way, they can guarantee the maintenance of their energy requirements for cellular processes, growth, and motility when experiencing light limitation during burying within migrating ripples.

4.2. Contrasting Migrating Ripple Effects on Phototrophs and Heterotrophs

The effect of ripple migration differed between phototrophs and heterotrophs. Regarding our second hypothesis, we expected phototrophs to be more affected by mechanical stress of migrating ripples than bacteria due to their larger cell size and dependency on light availability. In sandy reaches with sediment transport, metabolism is dominated by heterotrophic processes (Marcarelli et al., 2015; Uehlinger et al., 2002). While our results underline the negative effect of ripple migration, that is, mechanical stress, on bacterial abundance (phases 1 and 2) and bacterial production (phase 2), the phototrophic descriptors Chl *a* and fucoxanthin were not affected by sediment transport in phase 1, and peaked when stationary sediments became migrating (phase 2). This increase in pigments under migration in phase 2 cooccurred with increased net community production. We attribute this result to two factors. First, in our microcosms, drift was excluded. If the resistant diatoms were detached from sand grains and not broken, they still remain in the system contributing to metabolism. Second, pigment production per individual cell is increased under light limitation (Bogorad, 1962). In this way, the cell will guarantee sufficient light for maintaining the energy demand of cellular processes. Hence, changes in the pigment concentration in our sediments may not mirror changes in phototroph abundance or activity but may be rather an indicator of light conditions.

4.3. Microbial Response Modulated by Transition of Sediment Transport Regime (Phase 1 vs. 2)

Our third hypothesis stated that microbial metabolism would decrease when sediment transport is resumed and would increase when migration stopped. Although our data show that sediment transport regime transition influenced the microbial communities, the response is not the one that we predicted and more complex patterns emerged. Fast recovery of microbial communities was expected in response to the absence of mechanical stress and increase in "habitable" area (see above). Surprisingly, we observed that overall the differences from phase 1 were maintained in phase 2 regardless of the change in mechanical stress and associated stressors (light, "habitable" area); in other words, migrating sediments during phase 2 had comparable metabolism to stationary ones during phase 1 and vice versa. We suggest that this unexpected response results from a combination of the sediment transport history and the developmental stage of the microbial community. On the one hand, the microbial community after the transition had already experienced a history of certain sediment transport conditions. The initial sediment transport conditions (i.e., migrating ripple and stationary) in phase 1 determined the response of the microbial community in phase 2. This implies that the antecedent sediment transport conditions that a community experienced (phase 1) could have played a role in shaping the community response after transport transition (phase 2). On the other hand, the response of the microbial community to mechanical stress and light limitation depends on their development stage, as known from streambed scouring (Peterson et al., 1990; Sousa, 1980). The conditions under which the community developed determined the metabolism and was maintained in the following phase. Therefore, the effect of sediment transport is key to communities in an early developmental stage but seems to be overridden as the community becomes more mature. Further research could include more transitions and different sediment turnover rates. The response of microbial communities may depend on how fast and for how long the ripples migrate. As an example, faster sediment turnover ($>1\ h^{-1}$) and associated shorter resting times might affect communities that develop at stationary conditions more intensively and hampering metabolism as does ripple migration in early developmental stage. During an 8-h-period of ripple migration, bacterial and algal abundances were not reduced (D. C. Miller, 1989), while after 72 h of ripple migration metabolism was reduced by about 50% (Zlatanović et al., 2017). Therefore, understanding and upscaling the role of sediment transport at low flow on metabolism requires knowing not only the mechanisms acting over the biogeochemical processes but also the spatiotemporal dynamics of microbial communities and sediment transport.

5. Conclusions

Our results illustrate the importance of sediment transport at low flow for streambed metabolism. The hampering of the phototrophic (77%) and heterotrophic (40%) microbial activity, as consequence of sediment transport as migrating ripples, resulted from mechanical forces, light limitation, and reduced "habitable" area. Our results expand previous research to phototrophic communities, their activity is susceptible to sediment migration while their biomass remained unaffected. Further, the influence of sediment transport regime is conditioned by the antecedent sediment transport conditions as well as the developmental stage of the sediment community prior to the initiation/end of sediment transport. Both the effect of migration and transport timing may be considered when studying metabolism from sandy stream and river reaches. However, more research is needed to properly assess and incorporate the effect of sediment transport dynamics and its spatiotemporal variability to reach-scale patterns of metabolism.

Data Availability Statement

Following the FAIR data guidelines, all data presented will be available via the data repository www.pangaea.de (Scheidweiler, 2020) (doi.org/10.1594/PANGAEA.921544).

Acknowledgments
The study was financed by grants to M.M. (MU 1464/5-1 and MU 1464/7-1), C.M.-L. (grant BFI 09.338 by Basque Country Government), and U.R.-B. (RI 2093/2-1). The authors have no conflicts of interests. We like to thank T. Wolburg, G. Lippert, J. Rücker, and K. Lerche for technical support and M. Knie, A. Dolman, and S. Zlatanović for fruitful discussions.

References

Ahmerkamp, S., Marchant, H. K., Peng, C., Probandt, D., Littmann, S., Kuypers, M. M. M., & Holtappels, M. (2020). The effect of sediment grain properties and porewater flow on microbial abundance and respiration in permeable sediments. *Scientific Reports*, *10*(1), 3573. https://doi.org/10.1038/s41598-020-60557-7

Ahmerkamp, S., Winter, C., Janssen, F., Kuypers, M. M. M., & Holtappels, M. (2015). The impact of bedform migration on benthic oxygen fluxes. *Journal of Geophysical Research: Biogeosciences*, *120*, 2229–2242. https://doi.org/10.1002/2015JG003106

Ahmerkamp, S., Winter, C., Kramer, K., de Beer, D., Janssen, F., Friedrich, J., et al. (2017). Regulation of benthic oxygen fluxes in permeable sediments of the coastal ocean. *Limnology & Oceanography*, *62*(5), 1935–1954. https://doi.org/10.1002/lno.10544

Atkinson, B. L., Grace, M. R., Hart, B. T., & Vanderkruk, K. E. N. (2008). Sediment instability affects the rate and location of primary production and respiration in a sand-bed stream. *Journal of the North American Benthological Society*, *27*(3), 581–592. https://doi.org/10.1899/07-143.1

Attermeyer, K., Premke, K., Hornick, T., Hilt, S., & Grossart, H. P. (2013). Ecosystem-level studies of terrestrial carbon reveal contrasting bacterial metabolism in different aquatic habitats. *Ecology*, *94*(12), 2754–2766. https://doi.org/10.1890/13-0420.1

Baas, J. H. (1993). Dimensional analysis of current ripples in recent and ancient depositional environments. *Geologica Ultraiectina*, *106*, pp. 199.

Baas, J. H. (1999). An empirical model for the development and equilibrium morphology of current ripples in fine sand. *Sedimentology*, *46*(1), 123–138. https://doi.org/10.1046/j.1365-3091.1999.00206.x

Baas, J. H. (2003). Ripple, ripple mark, and ripple structure. In V.Middleton (Ed.), *Encyclopedia of sediments & sedimentary rocks* (pp. 565–567). Bodmin, Cornwall, UK: Springer.

Bates, D., Machler, M., Bolker, B. M., & Walker, S. C. (2015). Fitting linear mixed-effects models using lme4. *Journal of Statistical Software*, *67*(1), 1–48. https://doi.org/10.18637/jss.v067.i01

Battin, T. J., Besemer, K., Bengtsson, M. M., Romaní, A. M., & Packmann, A. I. (2016). The ecology and biogeochemistry of stream biofilms. *Nature Reviews Microbiology*, *14*(4), 251–263. https://doi.org/10.1038/nrmicro.2016.15

Battin, T. J., Luyssaert, S., Kaplan, L. A., Aufdenkampe, A. K., Richter, A., & Tranvik, L. J. (2009). The boundless carbon cycle. *Nature Geoscience*, *2*(9), 598–600. https://doi.org/10.1038/ngeo618

Biggs, B. J. F., Nikora, V. I., & Snelder, T. H. (2005). Linking scales of flow variability to lotic ecosystem structure and function. *River Research and Applications*, *21*(2–3), 283–298. https://doi.org/10.1002/rra.847

Bogorad, L. (1962). Chlorophylls. In R. A.Lewin (Ed.), *Physiology and biochemistry of algae* (pp. 385–408). New York: Academic Press Inc.

Booker, D. J., & Dunbar, M. J. (2008). Predicting river width, depth and velocity at ungauged sites in England and Wales using multilevel models. *Hydrological Processes: International Journal*, *22*(20), 4049–4057. https://doi.org/10.1002/hyp.7007

Bridge, J. S. (2003). *Rivers and floodplains. Forms, processes, and sedimentary record* (1st ed.). Oxford, UK: Blackwell Science.

Buesing, N., & Gessner, M. O. (2006). Benthic bacterial and fungal productivity and carbon turnover in a freshwater marsh. *Applied and Environmental Microbiology*, *72*(1), 596–605. https://doi.org/10.1128/AEM.72.1.596–605.2006

Charru, F., Andreotti, B., & Claudin, P. (2013). Sand ripples and dunes. *Annual Review of Fluid Mechanics*, *45*, 469–493. https://doi.org/10.1146/annurev-fluid-011212-140806

Cohn, S. A., & Weitzell, R. E. (1996). Ecological considerations of diatom cell motility. 1. Characterization of motility and adhesion in four diatom species. *Journal of Phycology*, *32*(6), 928–939. https://doi.org/10.1111/j.0022-3646.1996.00928.x

Consalvey, M., Paterson, D. M., & Underwood, G. J. C. (2004). The ups and downs of life in a benthic biofilm: Migration of benthic diatoms. *Diatom Research*, *19*(2), 181–202. https://doi.org/10.1080/0269249X.2004.9705870

Delgado, M., De Jonge, V. N., & Peletier, H. (1991). Effect of sand movement on the growth of benthic diatoms. *Journal of Experimental Marine Biology and Ecology*, *145*, 221–231. https://doi.org/10.1016/0022-0981(91)90177-X

Dickman, M. D., Peart, M. R., & Yim, W. W. S. (2005). Benthic diatoms as indicators of stream sediment concentration in Hong Kong. *International Review of Hydrobiology*, *90*(4), 412–421. https://doi.org/10.1002/iroh.200410806

Elliot, A. H., & Brooks, N. H. (1997). Transfer of nonsorbing solutes to a streambed with bed forms: Theory. *Water Resources Research*, *33*(1), 23–136. https://doi.org/10.1029/96WR02784

Espeland, E. M., & Wetzel, R. G. (2001). Effects of photosynthesis on bacterial phosphatase production in biofilms. *Microbial Ecology*, *42*, 328–337. https://doi.org/10.1007/s002480000117

Fischer, H., Kloep, F., Wilzcek, S., & Pusch, M. T. (2005). A river's liver—Microbial processes within the hyporheic zone of a large lowland river. *Biogeochemistry*, *76*(2), 349–371. https://doi.org/10.1007/s10533-005-6896-y

Flemming, H. C., Wingender, J., Szewzyk, U., Steinberg, P., Rice, S. A., & Kjelleberg, S. (2016). Biofilms: An emergent form of bacterial life. *Nature Reviews Microbiology*, *14*(9), 563–575. https://doi.org/10.1038/nrmicro.2016.94

Hart, D. D., & Finelly, C. M. (1999). Physical–biological coupling in streams: The pervasive effects of flow on benthic organisms. *Annual Review of Ecology and Systematics*, *30*, 363–395. https://doi.org/10.1146/annurev.ecolsys.30.1.363

Harvey, J. W., Drummond, J. D., Martin, R. L., McPhillips, L. E., Packman, A. I., Jerolmack, D. J., et al. (2012). Hydrogeomorphology of the hyporheic zone: Stream solute and fine particle interactions with a dynamic streambed. *Journal of Geophysical Research*, *117*, G00N11. https://doi.org/10.1029/2012JG002043

Hay, S. I., Maitland, T. C., & Paterson, D. M. (1993). The speed of diatom migration through natural and artificial substrata. *Diatom Research*, *8*(2), 371–384. https://doi.org/10.1080/0269249X.1993.9705268

Hoellein, T. J., Tank, J. L., Rosi-Marshall, E. J., & Entrekin, S. A. (2009). Temporal variation in substratum-specific rates of N uptake and metabolism and their contribution at the stream-reach scale. *Journal of the North American Benthological Society*, *28*(2), 305–318. https://doi.org/10.1899/08-073.1

Hünken, A., & Mutz, M. (2007). Field studies on factors affecting very fine and ultra fine particulate organic matter deposition in low-gradient sand-bed streams. *Hydrological Processes*, *21*(4), 525–533. https://doi.org/10.1002/hyp.6263

Izagirre, O., Serra, A., Guasch, H., & Elosegi, A. (2009). Effects of sediment deposition on periphytic biomass, photosynthetic activity and algal community structure. *The Science of the Total Environment*, *407*(21), 5694–5700. https://doi.org/10.1016/j.scitotenv.2009.06.049

Jewson, D. H., Lowry, S. F., & Bowen, R. (2006). Co-existence and survival of diatoms on sand grains. *European Journal of Phycology*, *41*(2), 131–146. https://doi.org/10.1080/09670260600652903

Kamp, A., de Beer, D., Nitsch, J. L., Lavik, G., & Stief, P. (2011). Diatoms respire nitrate to survive dark and anoxic conditions. *Proceedings of the National Academy of Sciences of the United States of America*, *108*(14), 5649–5654. https://doi.org/10.1073/pnas.1015744108

Kaufman, M. H., Cardenas, M. B., Buttles, J., Kessler, A. J., & Cook, P. L. M. (2017). Hyporheic hot moments: Dissolved oxygen dynamics in the hyporheic zone in response to surface flow perturbations. *Water Resources Research*, *53*, 6642–6662. https://doi.org/10.1002/2016WR020296

Kohl, J.-G., & Nicklisch, A. (1988). *Ökophysiologie der Algen. Wachstum und Ressourcennutzung* (253 pp.). Berlin, Germany: Akademie-Verlag Berlin.

Krejci, M. E., & Lowe, R. L. (1986). Importance of sand grain mineralogy and topography in determining micro-spatial distribution of epipsammic diatoms. *Journal of the North American Benthological Society*, *5*(3), 211–220. https://doi.org/10.2307/1467708

Leeder, M. R. (1982). *Sedimentology: Process and product*. The Netherlands: Springer.

Lenth, R. V. (2020). *emmeans: Estimated marginal means, aka least-squares means, R package version 1.4.4*. https://CRAN.R-project.org/package=emmeans

Leopold, L. B., Wolman, M. G., & Miller, J. P. (1964). *Fluvial processes in geomorphology* (535 pp.). Mineola, NY: Dover Publications.

Lewin, J. C., & Lewin, R. A. (1960). Autotrophy and heterotrophy in marine littoral diatoms. *Canadian Journal of Microbiology*, *6*(2), 127–134. https://doi.org/10.1139/m60-015

Lichtman, I. D., Baas, J. H., Amoudry, L. O., Thorne, P. D., Malarkey, J., Hope, J. A., et al. (2018). Bedform migration in a mixed sand and cohesive clay intertidal environment and implications for bed material transport predictions. *Geomorphology*, *315*, 17–32. https://doi.org/10.1016/j.geomorph.2018.04.016

Macedo, M. F., Ferreira, J. G., & Duarte, P. (1998). Dynamic behavior of photosynthesis–irradiance curves determined from oxygen production during variable incubation periods. *Marine Ecology Progress Series*, *165*, 31–43. https://doi.org/10.3354/meps165031

Marcarelli, A. M., Huckins, C. J., & Eggert, S. L. (2015). Sand aggradation alters biofilm standing crop and metabolism in a low-gradient Lake Superior tributary. *Journal of Great Lakes Research*, *41*(4), 1052–1059. https://doi.org/10.1016/j.jglr.2015.09.004

Mendoza-Lera, C., Frossard, A., Knie, M., Federlein, L. L., Gessner, M. O., & Mutz, M. (2017). Importance of advective mass transfer and sediment surface area for streambed microbial communities. *Freshwater Biology*, *62*(1), 133–145. https://doi.org/10.1111/fwb.12856

Mendoza Lera, C., & Mutz, M. (2013). Microbial activity and sediment disturbance modulate the vertical water flux in sandy sediments. *Freshwater Science*, *32*(1), 26–38. https://doi.org/10.1899/11-165.1

Miller, A. R., Lowe, R. L., & Rotenberry, J. T. (1987). Succession of diatom communities on sand grains. *Journal of Ecology*, *75*(3), 693–709. https://doi.org/10.2307/2260200

Miller, D. C. (1989). Abrasion effects on microbes in sandy sediments. *Marine Ecology Progress Series*, *55*(1), 73–82. https://doi.org/10.3354/meps055073

Mutz, M., Schlief, J., & Orendt, C. (2001). *Morphologische Referenzzustände für Bäche im Land Brandenburg* (pp. 80). Potsdam, Germany: Landesumweltamt Brandenburg.

Nixdorf, B., & Jander, J. (2003). Bacterial activities in shallow lakes—A comparison between extremely acidic and alkaline eutrophic hard water lakes. *Hydrobiologia*, *506–509*, 697–705. https://doi.org/10.1023/B:HYDR.0000008623.73250.c8

O'Connor, B. L., Harvey, J. W., & McPhillips, L. E. (2012). Thresholds of flow-induced bed disturbances and their effects on stream metabolism in an agricultural river. *Water Resources Research*, *48*, W08504. https://doi.org/10.1029/2011WR011488

Paola, C., & Seal, R. (1995). Grain-size patchiness as a cause of selective deposition and downstream fining. *Water Resources Research*, *31*(5), 1395–1407. https://doi.org/10.1029/94WR02975

Peterson, C. G., Hoagland, K. D., & Stevenson, R. J. (1990). Timing of wave disturbance and the resistance and recovery of a fresh-water epilithic microalgal community. *Journal of the North American Benthological Society*, *9*(1), 54–67. https://doi.org/10.2307/1467934

Pilditch, C. A., & Miller, D. C. (2006). Phytoplankton deposition to permeable sediments under oscillatory flow: Effects of ripple geometry and resuspension. *Continental Shelf Research*, *26*(15), 1806–1825. https://doi.org/10.1016/j.csr.2006.06.002

Poff, N. L., Allan, J. D., Bain, M. B., Karr, J. R., Prestegaard, K. L., Richter, B. D., et al. (1997). The natural flow regime. *BioScience*, *47*, 769–784.

Probandt, D., Eickhorst, T., Ellrott, A., Amann, R., & Knittel, K. (2018). Microbial life on a sand grain: From bulk sediment to single grains. *The ISME Journal*, *12*(2), 623–633. https://doi.org/10.1038/ismej.2017.197

Rabení, C. F., Doisy, K. E., & Zweig, L. D. (2005). Stream invertebrate community functional responses to deposited sediment. *Aquatic Sciences*, *67*(4), 395–402. https://doi.org/10.1007/s00027-005-0793-2

R Core Team. (2018). *R: A language and environment for statistical computing*. Vienna, Austria: R Foundation for Statistical Computing. https://www.R-project.org/

Risse-Buhl, U., Anlanger, C., Chatzinotas, A., Noss, C., Lorke, A., & Weitere, M. (2020). Near streambed flow shapes microbial guilds within and across trophic levels in fluvial biofilms. *Limnology & Oceanography*, *65*(10), 2261–2277. https://doi.org/10.1002/lno.11451

Risse-Buhl, U., Anlanger, C., Kalla, K., Neu, T. R., Noss, C., Lorke, A., & Weitere, M. (2017). The role of hydrodynamics in shaping the composition and architecture of epilithic biofilms in fluvial ecosystems. *Water Research*, *127*, 211–222. https://doi.org/10.1016/j.watres.2017.09.054

Risse-Buhl, U., Felsmann, K., & Mutz, M. (2014). Colonization dynamics of ciliate morphotypes modified by shifting sandy sediments. *European Journal of Protistology*, *50*, 345–355. https://doi.org/10.1016/j.ejop.2014.03.006

Roberts, S., Sabater, S., & Beardall, J. (2004). Benthic microalgal colonization in streams of differing riparian cover and light availability. *Journal of Phycology*, *40*(6), 1004–1012. https://doi.org/10.1111/j.1529-8817.2004.03-333.x

Romaní, A. M., & Sabater, F. (2000). Influence of algal biomass on extracellular enzyme activity in river biofilms. *Microbial Ecology*, *41*, 16–24. https://doi.org/10.1007/s002480000041

Rutherford, J. C., Latimer, G. J., & Smith, R. K. (1993). Bedform mobility and benthic oxygen uptake. *Water Research*, *27*(10), 1545–1558. https://doi.org/10.1016/0043-1354(93)90099-4

Rutherford, J. C., Wilcock, R. J., & Hicker, C. W. (1991). Deoxygenation in a mobile-bed river—I. Field studies. *Water Research*, *25*(12), 1487–1497. https://doi.org/10.1016/0043-1354(91)90179-T

Savant, A. S., Reible, D. O., & Thibodeaux, L. J. (1987). Convective transport within stable river sediments. *Water Resources Research*, *23*(9), 1763–1768. https://doi.org/10.1029/WR023i009p01763

Scheidweiler, D., Mendoza-Lera, C., Mutz, M., & Risse-Buhl, U. (2020). Metabolism, nutrient dynamics and community composition in sandy sediments - A microcosms experiment. PANGAEA, https://doi.org/10.1594/PANGAEA.921544

Scheidweiler, D., Peter, H., Pramateftaki, P., de Anna, P., & Battin, T. J. (2019). Unraveling the biophysical underpinnings to the success of multispecies biofilms in porous environments. *The ISME Journal*, *13*(7), 1700–1710. https://doi.org/10.1038/s41396-019-0381-4

Sekar, R., Nair, K. V. K., Rao, V. N. R., & Venugopalan, V. P. (2002). Nutrient dynamics and successional changes in a lentic freshwater biofilm. *Freshwater Biology*, *47*(10), 1893–1907. https://doi.org/10.1046/j.1365-2427.2002.00936.x

Shimeta, J., Amos, C. L., Beaulieu, S. E., & Ashiru, O. M. (2002). Sequential resuspension of protists by accelerating tidal flow: Implications for community structure in the benthic boundary layer. *Limnology & Oceanography*, *47*(4), 1152–1164. https://doi.org/10.4319/lo.2002.47.4.1152

Singh, S. K., Pahlow, M., Booker, D. J., Shankar, U., & Chamorro, A. (2019). Towards baseflow index characterization at national scale in New Zealand. *Journal of Hydrology*, *568*, 646–657. https://doi.org/10.1016/j.jhydrol.2018.11.025

Sinsabaugh, R. L., Shah, J. J. F., Findlay, S. G., Kuehn, K. A., & Moorhead, D. L. (2015). Scaling microbial biomass, metabolism and resource supply. *Biogeochemistry*, *122*(2–3), 175–190. https://doi.org/10.1007/s10533-014-0058-z

Smakhtin, V. U. (2001). Low flow hydrology: A review. *Journal of Hydrology*, *240*(3–4), 147–186. https://doi.org/10.1016/S0022-1694(00)00340-1

Sobczak, W. V. (1996). Epilithic bacterial responses to variations in algal biomass and labile dissolved organic carbon in water. *Journal of the North American Benthological Society*, *15*(2), 143–154. https://doi.org/10.2307/1467944

Sousa, W. P. (1980). The responses of a community to disturbance—The importance of successional age and species life histories. *Oecologia*, *45*(1), 72–81. https://doi.org/10.1007/BF00346709

Sukhodolov, A. N., Fedele, J. J., & Rhoads, B. L. (2006). Structure of flow over alluvial bedforms: An experiment on linking field and laboratory methods. *Earth Surface Processes and Landforms*, *31*(10), 1292–1310. https://doi.org/10.1002/esp.1330

Sutherland, A. B., Culp, J. M., & Benoy, G. A. (2010). Characterizing deposited sediment for stream habitat assessment. *Limnology and Oceanography: Methods*, *8*, 30–44. https://doi.org/10.4319/lom.2010.8.30

Uehlinger, U. (2000). Resistance and resilience of ecosystem metabolism in a flood-prone river system. *Freshwater Biology*, *45*, 319–332. https://doi.org/10.1111/j.1365-2427.2000.00620.x

Uehlinger, U., Naegeli, M., & Fisher, S. G. (2002). A heterotrophic desert stream? The role of sediment stability. *Western North American Naturalist*, *62*(4), 466–473.

Verdonschot, P. F. M. (2001). Soft-bottomed lowland streams: A dynamic desert. *Proceedings of the International Association of Theoretical and Applied Limnology*, *27*, 2577–2581.

Verzano, K., Bärlund, I., Flörke, M., Lehner, B., Kynast, E., Voß, F., & Alcamo, J. (2012). Modeling variable river flow velocity on continental scale: Current situation and climate change impacts in Europe. *Journal of Hydrology*, *424*, 238–251. https://doi.org/10.1016/j.jhydrol.2012.01.005

Villanova, V., Fortunato, A. E., Singh, D., Dal Bo, D., Conte, M., Obata, T., et al. (2017). Investigating mixotrophic metabolism in the model diatom *Phaeodactylum tricornutum*.*Philosophical Transactions of the Royal Society B: Biological Sciences*, *372*(1728). https://doi.org/10.1098/rstb.2016.0404

Vincent, W. F., & Goldman, C. R. (1980). Evidence for algal heterotrophy in Lake-Tahoe, California–Nevada. *Limnology and Oceanography*, *25*(1), 89–99. https://doi.org/10.4319/lo.1980.25.1.0089

Wallbrink, P. J. (2004). Quantifying the erosion processes and land-uses which dominate fine sediment supply to Moreton Bay, Southeast Queensland, Australia. *Journal of Environmental Radioactivity*, *76*(1–2), 67–80. https://doi.org/10.1016/j.jenvrad.2004.03.019

Weise, W., & Rheinheimer, G. (1978). Scanning electron microscopy and epifluorescence investigation of bacterial colonization of marine sand sediments. *Microbial Ecology*, *4*(3), 175–188. https://doi.org/10.1007/BF02015075

Wickham, H. (2009). *ggplot2: Elegant graphics for data analysis*. New York: Springer.

Wilczek, S., Fischer, H., Brunke, M., & Pusch, M. T. (2004). Microbial activity within a subaqueous dune in a large lowland river (River Elbe, Germany). *Aquatic Microbial Ecology*, *36*(1), 83–97. https://doi.org/10.3354/ame036083

Wolke, P., Teitelbaum, Y., Deng, C., Lewandowski, J., & Arnon, S. (2020). Impact of bed form celerity on oxygen dynamics in the hyporheic zone. *Water*, *12*(1), 62. https://doi.org/10.3390/w12010062

Wood, P. J., & Armitage, P. D. (1997). Biological effects of fine sediment in the lotic environment. *Environmental Management*, *21*(2), 203–217. https://doi.org/10.1007/s002679900019

Zheng, L. Z., Cardenas, M. B., Wang, L. C., & Mohrig, D. (2019). Ripple effects: Bed form morphodynamics cascading into hyporheic zone biogeochemistry. *Water Resources Research*, *55*, 7320–7342. https://doi.org/10.1029/2018WR023517

Zlatanović, S., Fabian, J., Mendoza-Lera, C., Woodward, K. B., Premke, K., & Mutz, M. (2017). Periodic sediment shift in migrating ripples influences benthic microbial activity. *Water Resources Research*, *53*, 4741–4755. https://doi.org/10.1002/2017WR020656